

A Calibration Strategy for Systems with 2-D Laser Sensors

T. Dunker, S. Sperling, Fraunhofer IFF, Magdeburg

Abstract:

We consider measuring machines (MMs), which use one or more 2-D laser sensors (2-DLSs) for automated dimensional inspection. In order to transform several measurements from their sensor coordinate frame (CF) into a world or object CF, we need a parameterized model of these transformations. We present a method, which allows for very different MMs to set up a model, to construct a calibration object and to estimate the model parameter from measurements on the calibration object.

State of the Art

There exists a wide choice of commercially available sensors¹, which generate 2-D profile measurements observing a laser stripe projection on the surface of an object, see Fig. 1. As there is no unified terminology (laser stripe, light section, line structured-light, laser triangulation, etc.) let us call them 2-D laser sensors. Most frequently they are used for inspection tasks, which are restricted to relative measurements on a single profile like e.g. in weld seam, adhesive beading or gap inspection.

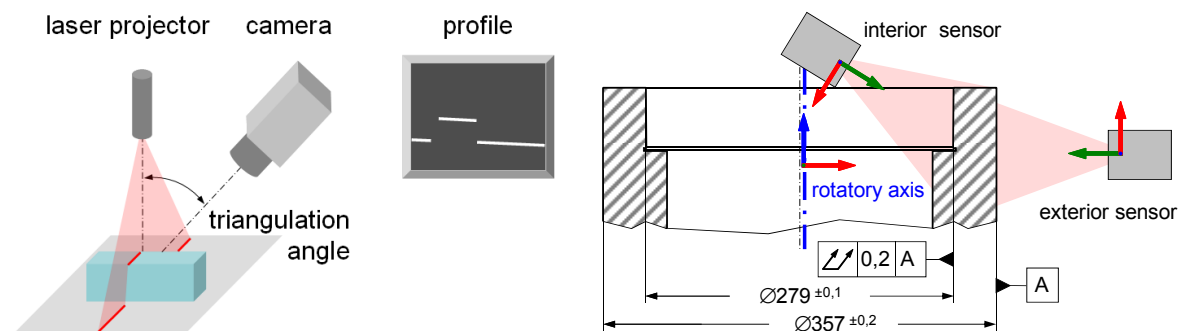


Fig. 1: Measurement principle of 2-DLSs (left) and example inspection task illustrating the need of calibrating the transformations between the CFs of sensors and axis (right)

¹ Automation Technology, Keyence, MEL, Micro-Epsilon, Omron, SmartRay and others provide 2-DLS for industrial automation. DATAPIXEL, Nikon, Perceptron, Zeiss and others have 2-DLS for CMMs in their portfolio.

Inspection applications using multiple profile measurements from a 2-DLS combined with motion axes or other 2-DLSs are less frequent. Exceptions are coordinate measuring machines (CMMs). In order to transform all profiles into a common CF one needs to calibrate the system of axes and 2-DLSs. For measurement volumes spanned by three orthogonal calibrated axes X-Y-Z one can use a method established for CMMs, which obtains the six position parameter of the 2-DLS from a sequence of measurements on a satin finished calibration sphere, see e.g. [1]. In the fields of computer vision and robotics there exist methods for calibrating laser scanner with respect to cameras using planar calibration targets, see e.g. [2]. This idea could be translated to 2-DLSs measuring planar calibration objects of different but known orientations.

What about the calibration of other configurations of 2-DLSs and axes like in Fig. 1? Do we need to develop a calibration method for each new configuration? In this paper we want to show that the method could always be the same, only the calibration object needs adaptations.

A unified calibration approach

Let us consider a MM with some configuration of 2-DLS and axes. We wish that the calibration procedure consists only in a sequence of measurements on a suitable calibration object placed in the MM. For a given MM, we define local CFs of 2-DLSs, axes and calibration object and model transformations between them as joints, which results in a model of the MM kinematic, see Fig. 2. Remark, that the calibration object is decomposed into basic geometric objects.

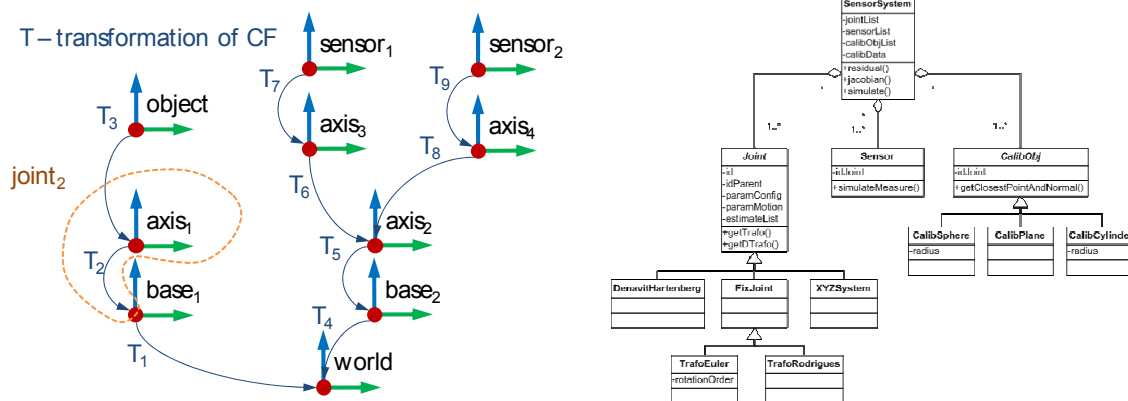


Fig. 2: Tree structure of local CFs and transformations (left) and derived class model for MMs (SensorSystem) and their components

The transformations – rotation R and translation by a vector t – inside each joint can be represented by a homogenous 4x4 matrix

$$T = \begin{pmatrix} R & t \\ 0 & 1 \end{pmatrix}.$$

Let $X_{m,i}^s$ be the i -th point of the m -th measurement by sensor s . Let this point be situated on basic geometric object o . Parameters of the joints, which are not precisely known e.g. because of assembly tolerances, are collected into a vector p . Transformation T_j of joint j depends only on few or no components p_j from p , on some fixed parameters f_j and on motion parameters $b_{m,j}$ of measurement m . Then the transformation between the CFs of the object o and the world during the m -th measurement can be written as

$$T_m^o(p) = T_{j_1}(p_{j_1}, f_{j_1}, b_{m,j_1}) \cdots T_{j_k}(p_{j_k}, f_{j_k}, b_{m,j_k}),$$

where j_1, \dots, j_k denotes the chain of joints between object and world. Analogously let $T_m^s(p)$ denote the transformation between the CFs of sensor s and the world during measurement m . Hence we can transform a measured point to the CF of the corresponding object

$$\tilde{X}_{m,i}^s = (T_m^o(p))^{-1} T_m^s(p) X_{m,i}^s.$$

Let $c^o: \mathbb{R}^3 \rightarrow S^o \subset \mathbb{R}^3$ be the function, which maps each point in the CF of object o to the closest point on its surface S^o . Furthermore, denote by $n^o: S^o \rightarrow \{x: x \in \mathbb{R}^3, \|x\| = 1\}$ the function returning the outer normal. We define for each $X_{m,i}^s$ the residual as signed distance between $X_{m,i}^s$ and the object o by

$$r_{m,i}^s(p) = n^o(c^o(\tilde{X}_{m,i}^s))^T \cdot (\tilde{X}_{m,i}^s - c^o(\tilde{X}_{m,i}^s)).$$

We estimate the unknown parameter p by solving the non-linear least square problem

$$f(p) = \frac{1}{2} \sum_m \sum_s \sum_i (r_{m,i}^s(p))^2 \rightarrow \min.$$

As solver we use publicly available functions from the PORT library². These algorithms were described in [3]. The jacobian for the above defined residuals can be computed by

$$\frac{\partial r_{m,i}^s(p)}{\partial p_j} = n^o(c^o(\tilde{X}_{m,i}^s))^T \cdot \frac{\partial (T_m^o(p))^{-1} T_m^s(p)}{\partial p_j} X_{m,i}^s.$$

Tree structure, computation of transformations and derivatives, closest points and normals were mapped to an extensible class model, which permits to represent a wide range of MMs. If a model contains redundant parameters (more parameters than degrees of freedom) or is close to a singularity (small configuration changes correspond to large parameter changes – e.g. longitude close to a pole) the parameter estimate will fail. E.g. two successive Denavit-

² <http://www.netlib.org/port/>

Hartenberg joints for almost parallel axis would yield a singular parameterization, which can be avoided by inserting an auxiliary fixed joint.

Planes, cylinder and spheres are used as basic geometric objects for the construction of calibration objects. They can be manufactured with small form tolerance. Closest points and normals can be computed in closed form – no iterations necessary. They should be satin finished in order to obtain best possible measurement conditions. Once a calibration object is manufactured, the positions of the basic geometric objects are determined on a CMM. Design of calibration object and planning the measurements on it go hand in hand (visibility, collision avoidance). Let us call both together calibration strategy (CS). Its result will determine the set of expected measurement points. It must be checked that small changes of unknown parameters cause detectable changes in the measurement points. Fig. 3 illustrates how the design of the calibration object influences the sensitivity of the measurement with respect to changes of the unknown parameter. As the situation might be fairly complex, we included simulation in our model for analysis and verification of CSs.

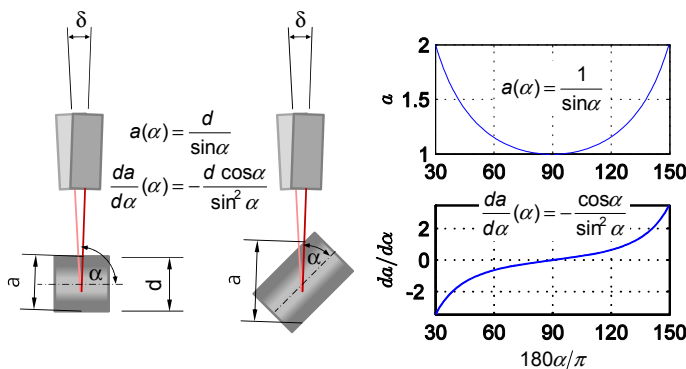


Fig. 3: If a cylinder is placed orthogonally with respect to the assumed plane of measurement, an out-of-plane-error of $\delta = 1^\circ$ causes a change of 0.02% of the major axis a . Measuring a 45° inclined cylinder the same error $\delta = 1^\circ$ changes a by 1.7%.

Residuals and covariance allow analysing the result of a parameter estimate. Residuals corresponding to one basic geometric object should be symmetrically distributed around the surface, see Fig. 4. Deviations from this ideal situation might reveal measurement errors depending on the surface orientation, deviations from the ideal motion, synchronization errors, wrong CMM data assignment or others. Not symmetrically distributed residuals corresponding to one sensor might be caused by some lateral scaling error of the sensor, by positioning error of axis without a scale (e.g. backlash) or by others.

The solver returns together with the optimal parameter $p^* \in \mathbb{R}^{n_p}$ a $n_p \times n_p$ covariance matrix $\Xi = \sigma^2 H^{-1} (J^T J) H^{-1}$, where $\sigma^2 = 2f(p^*) / (n_m - n_p)$ is the variance, the $n_p \times n_p$ matrix H is a finite differences approximation of the hessian $\nabla^2 f(p^*)$ and the $n_m \times n_p$ matrix

$$J = \left(\frac{\partial r_{m,i}^s(p^*)}{\partial p_j} \right)_{(m,s,i),j}$$

denotes the jacobian of the residuals. The estimated p^* may be interpreted as sum of the “true” parameter and a random vector with zero mean and covariance Ξ , see e.g. [4]. Assuming normality and neglecting correlations parameter p_i lies in the confidence interval $[p_i^* - 2.576\sqrt{\Xi_{i,i}}, p_i^* + 2.576\sqrt{\Xi_{i,i}}]$ with 99% confidence level. Consequently, greater values $\sqrt{\Xi_{i,i}}$ might be a hint that changes of p_i do not cause changes in the measurements, which can be distinguished from the speckle noise (e.g. to few measurement points for filtering average effects) or are of the same magnitude as other parameters.

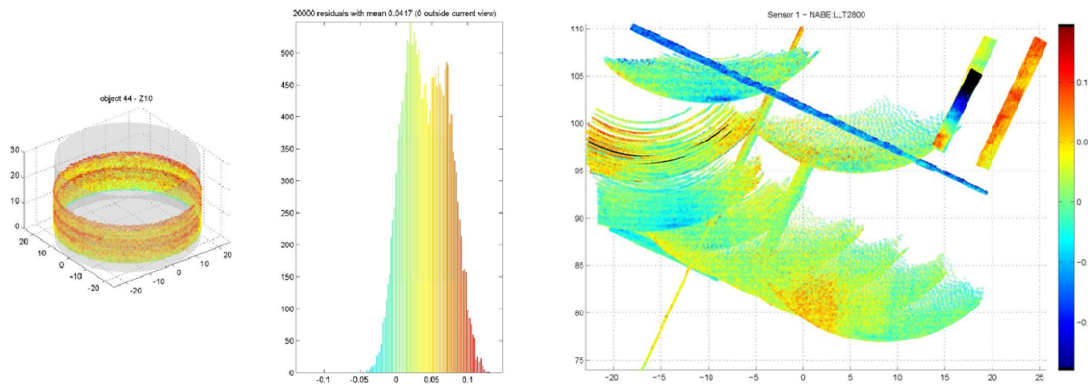


Fig. 4: Example for analysis of residuals corresponding to a basic geometric object (left) or to one sensor (right) with color coded magnitude and histogram for symmetry considerations

An application example

A MM from ASCONA GmbH for automated dimensional inspection of bead seat, central and bolt holes of machined alloy wheels serves as an example for evaluating the proposed calibration approach, see Fig. 5. This MM has three 2-DLS for inner and outer bead seat and central hole and one 1-DLS for the calottes or cones of the bolt holes. The sensors are turned around the centered and clamped wheel. Several axes for positioning the sensors permit the measurement of wheels with diameter from 13" to 24.5" and width from 3.5" to 17". As orthogonality and parallelism of the axes have considerable tolerances there are 39 degrees of freedom of the MM to be estimated. The calibration object needs to resemble a

wheel as the measurement volume consists of toroidal regions. We added a second outer “bead seat”, spheres and a second “central hole” feature, see Fig. 5. The position of the calibration object adds 6 further degrees of freedom to the model of the MM.

Using several measurements with different axes positions we can estimate the 39 machine parameter. Analyzing the residuals we discovered e.g. a lateral scaling error of the 2-DLS for the central hole, which could be corrected by recalibrating the 2-DLS. With the finally estimated parameter all measurement can be transformed into an object CF. Fig. 5 shows a resulting 3-D point set. It is the input to software, which automatically computes the features to be inspected like diameter, roundness, concentricity and runout, see [5]. This reference reports also a different calibration method, which is based on some assumptions on the alignment of axes and 2-DLS. This very specialized method uses a simpler calibration object and has less degree of freedom.

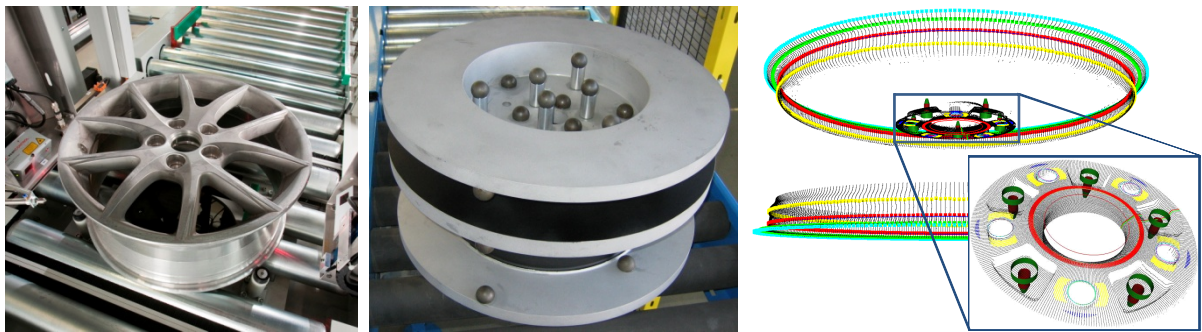


Fig. 5: MM for machined alloy wheels (left), wheel-like calibration object with second bead seat and additional spheres (middle) and 3-D point set (right) with automatically extracted features for inspecting diameters, runout, etc.

- [1] Xiong, H. Y., Xu, Y., Zong, Z. J.: Accurate extrinsic calibration method of line structured-light sensor based on standard ball. IEEE International Workshop on Imaging Systems and Techniques, Shenzhen 2009, pp 193-197
- [2] Gao, Z., Zhong, S., Zhang, W., Zhu, Y.: A high-precision calibration technique for laser measurement instrument and stereo vision sensors. 8th International Conference on Electronic Measurement & Instruments, Xi'an 2007, pp 214-217
- [3] Dennis, J., Gay, D., Welsch, R.: An adaptive nonlinear least-squares algorithm. ACM Transactions on Mathematical Software (7) Nr.3, 1981, pp 348-368
- [4] Curtis, A. R.: Analysis of covariance after nonlinear least-squares fitting. IMA Journal of Numerical Analysis (6), 1986, pp. 453-461
- [5] Teutsch, C., Berndt, D., Schmidt, N., Trostmann, E.: Automated geometry measurement of wheel rims based on optical 3D metrology. Two- and Three-Dimensional Methods for Inspection and Metrology IV, Boston 2006, paper 63820I